Endoplasmic reticulum–endosome contact increases as endosomes traffic and mature

Jonathan R. Friedman, Jared R. DiBenedetto, Matthew West, Ashley A. Rowland, and Gia K. Voeltz
Department of Molecular, Cellular, and Developmental Biology, University of Colorado, Boulder, CO 80309

ABSTRACT **The endosomal pathway is responsible for plasma membrane cargo uptake, sorting, and, in many cases, lysosome targeting. Endosome maturation is complex, requiring proper spatiotemporal recruitment of factors that regulate the size, maturity, and positioning of endosomal compartments. In animal cells, it also requires trafficking of endosomes on microtubules. Recent work has revealed the presence of contact sites between some endosomes and the endoplasmic reticulum (ER). Although these contact sites are believed to have multiple functions, the frequency, dynamics, and physical attributes of these contacts are poorly understood. Here we use high-resolution three-dimensional electron microscopy to reveal that ER tubules wrap around endosomes and find that both organelles contact microtubules at or near membrane contact sites. As endosomes traffic, they remain bound to the ER, which causes the tubular ER to rearrange its structure around dynamic endosomes at contact sites. Finally, as endosomes transition through steps of maturation, they become more tightly associated with the ER. The major implication of these results is that endosomes mature and traffic while coupled to the ER membrane rather than in isolation.**

Monitoring Editor
Ramanujan S. Hegde
National Institutes of Health

Received: Oct 11, 2012
Revised: Jan 7, 2013
Accepted: Jan 24, 2013

INTRODUCTION

Endocytosis is a mechanism used by eukaryotic cells to internalize components from the plasma membrane (PM) and the extracellular matrix. Endocytosis begins with the PM membrane being deformed into a vesicle that buds into the cytoplasm. After internalization, the endocytic vesicle becomes an early endosome (EE) as it accumulates Rab5 on its surface (Huotari and Helenius, 2011; Zeigerer *et al.*, 2012). Rab accumulation establishes endosomal identity and allows for the recruitment and regulation of factors that enable cargo sorting, endosomal fusion and fission, trafficking, and maturation (Stenmark, 2009). EEs that contain cargo destined for degradation at the lysosome will exchange Rab5 on their surface for Rab7 (Rink *et al.*, 2005; Poteryaev *et al.*, 2010). This Rab exchange marks the conversion of an EE into a more "mature" late endosome (LE). Endosome maturation is also accompanied by other changes that include endosome growth, acidification, and internalization of intralumenal vesicles (Huotari and Helenius, 2011). As endosomes mature along the degradative pathway, they must also traffic along the cytoskeleton in order for their cargo to reach the perinuclear lysosome (Nielsen *et al.*, 1999; Vonderheit and Helenius, 2005).

Recent evidence suggests that endosome maturation and trafficking might not occur in isolation along cytoskeletal tracks; there are several reports that endosomes form membrane contact sites with the endoplasmic reticulum (ER). Contact sites between endosomes and the ER membrane have been confirmed at a high resolution by electron microscopy (EM) in mammalian cells and between the vacuole and the ER in yeast (Rocha *et al.*, 2009; Eden *et al.*, 2010; West *et al.*, 2011). One proposed role for these sites is to allow the direct transfer of cholesterol between the ER and LEs (Rocha *et al.*, 2009). ER–endosome contacts could also provide sites where endocytic cargo could be modified by proteins

This article was published online ahead of print in MBoC in Press (http://www.molbiolcell.org/cgi/doi/10.1091/mbc.E12-10-0733) on February 6, 2013.

Address correspondence to: Gia K. Voeltz (gia.voeltz@colorado.edu).

Abbreviations used: EE, early endosome; ER, endoplasmic reticulum; FM, fluorescence microscopy; LE, late endosome; MT, microtubule; MVB, multivesicular body; PM, plasma membrane.

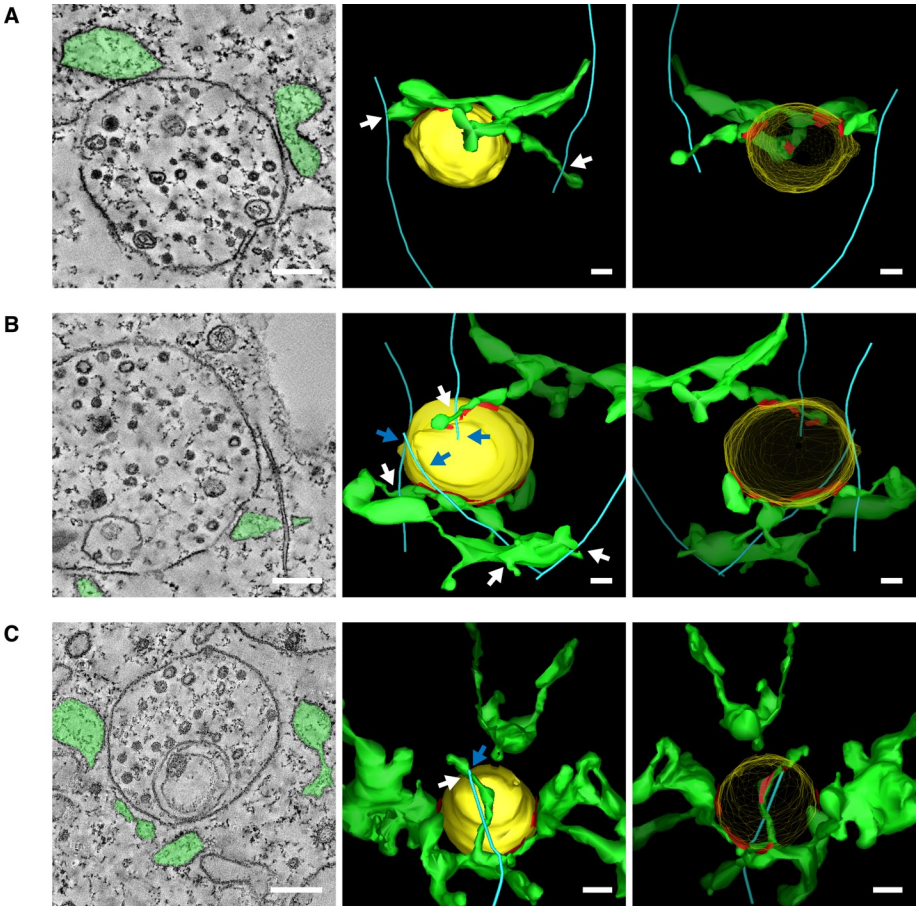

FIGURE 1: The 3D structure of contact sites between ER tubules, endosomes, and MTs is revealed by EM tomography in Cos-7 cells. (A–C) EM of high-pressure-frozen Cos-7 cells. EM tomographs (left) and 3D models are shown from forward (center) and reverse angles (right) (see Supplemental Videos S1–S3). The ER is shown in green, the endosomes are drawn in yellow, and MTs are shown in blue. Contact sites are defined as regions where the ER membrane comes within 30 nm of the endosomal membrane and ribosomes are excluded and are outlined in red on models. White arrows point to ER–MT contacts, and blue arrows point to endosomal–MT contacts. Scale bars, 200 nm.

localized to the ER membrane (Eden *et al.*, 2010; Stuible and Tremblay, 2010).

We recently reported examples of EEs that maintain contact with the ER over time by live confocal fluorescence microscopy (FM; Friedman *et al.*, 2010). These data introduced the possibility that ER–endosome contact might be sustained rather than transient. However, these data did not address the extent to which endosomes within a given population and/or at various stages of maturation associate with the ER membrane over time, nor did they determine the effect of endosome trafficking on ER contact. Here we use high-resolution EM to find that both the ER and endosomes contact microtubules (MTs) near their membrane contact sites, and this is likely to facilitate dynamic coupling between the ER and endosomes during trafficking. We determine that the ER predominantly rearranges its network of tubules in order to ensure maintained contact with dynamic endosomes. Finally, we demonstrate that endosomes become more tightly associated with the ER as they mature. The unexpectedly high degree of contact between maturing endosomes and the ER shows that endosomal maturation and trafficking is likely not autonomous and opens an exciting avenue of future research.

RESULTS

ER tubules wrap around endosomes, and both organelles bind microtubules

Images taken by confocal FM revealed that dynamic EEs are capable of maintaining contact with the ER tubular membrane network over time by sharing coupled movements that may occur along MTs (Friedman *et al.*, 2010). Although these experiments are striking, in that they suggest that the two organelles can sustain contact despite their movements, they do not resolve the extent to which the two organelles contact each other and whether one or both are bound to a MT. To visualize contacts between endosomes, ER, and MTs at high resolution, we performed EM serial tomography and generated three-dimensional (3D) reconstructions of wild-type, high-pressure-frozen Cos-7 cells. Using this technique, we were able to reconstruct >95, 75, and 55% of the volume of three different endosomes (clearly defined by their inclusion of intralumenal vesicles). We also reconstructed the ER membrane around the endosomes, as well as any organelle-contacting MTs present within the reconstructed area. We observed multiple cases in which a single multivesicular body (MVB) has multiple contacts with the ER membrane and appears "wrapped" by ER (Figure 1, A–C). In the first case (Figure 1A and Supplemental Video S1), ER tubules form a half-ring around the endosome, making three distinct contacts with it (ER in the model is colored green; contacting domains are red). In this example, the reconstructed endosomal membrane does not contact MTs, whereas the surrounding ER contacts two different MTs. This endosome might be an example of a nondynamic endosome that stays in contact with the ER as the ER moves around it. A second example (Figure 1B and Supplemental Video S2) shows an MVB contacted on two sides by different ER tubules. This MVB forms contacts with three MTs, two of which also make contact with the ER membrane in close proximity to the MVB contact. Strikingly, the tomogram reveals that the ER membrane clamps around the MT right next to the MVB contact site (Figure 1B, left). A final example (Figure 1C and Supplemental Video S3) reveals an MVB contacted at five different sites by ER tubules, as well as the tip of a MT that also contacts the ER at an ER–endosome–MT junction. Thus the ER and endosomes might form extensive contacts that are maintained by coordinated trafficking of both organelles along the MT cytoskeleton. Further, these data raise the intriguing possibility that some of the more complex types of ER dynamics are driven by stable contact with endosomes and coupled dynamics of the organelles along MTs.

Many EEs are tightly associated with the ER over time

Our EM images of EEs and the ER suggest that the two organelles form extensive contacts that might allow them to move together along the MT cytoskeleton. However, these experiments do not address the frequency of endosomal contact with the ER and the

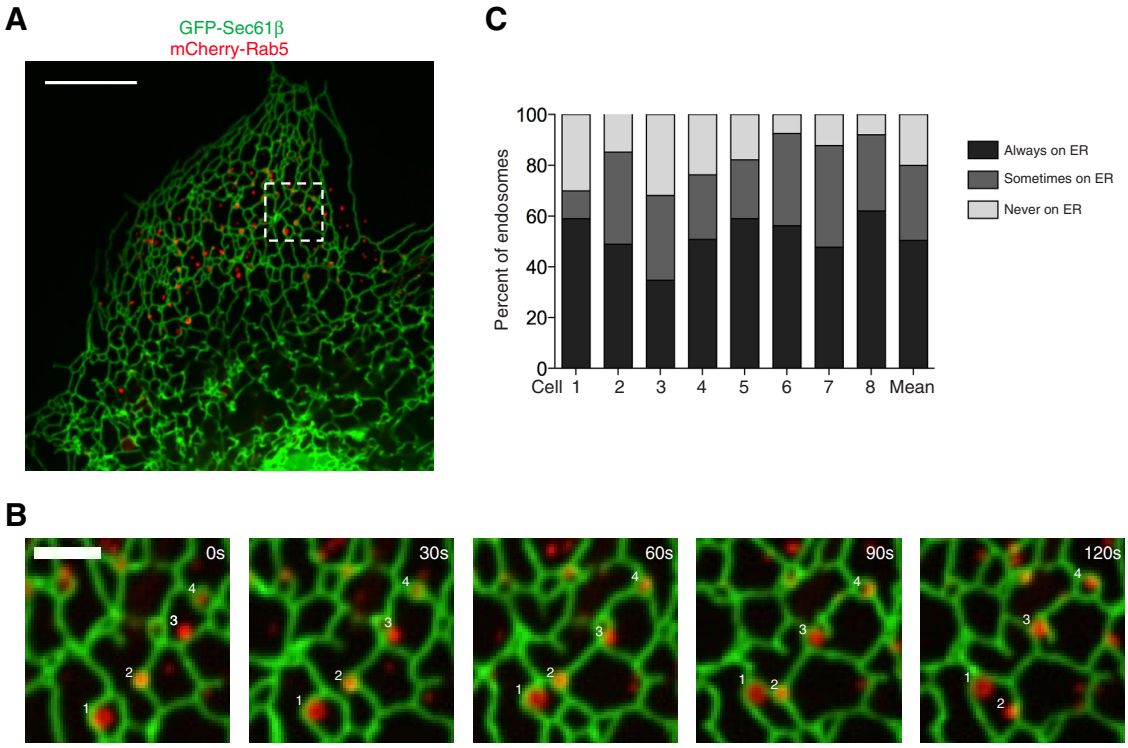

FIGURE 2: Many Rab5-labeled EEs are tightly associated with the ER membrane. (A) A representative merged image of a Cos-7 cell reveals the distribution of the ER membrane network relative to early endosomes (EEs; labeled with GFP-Sec61β and mCherry-Rab5, respectively). (B) A zoom-in of the dashed box in A over a 2-min time course tracks several endosomes that remain associated (examples 1, 2, and 4) or become associated (example 3) with the tubular ER during the course of the movie (see Supplemental Video S4). (C) A graph depicting the degree of contact between Rab5$^+$ EEs and the ER during 2-min movies (images taken 5 s apart). EEs were categorized as contacting the ER during the entire movie, part of the movie, or not at all. Data are shown from eight individual cells, as well as the mean value of contact based on the summation of the individual cell data ($n = 651$ endosomes). Scale bars, 10 μm (A), 2 μm (B).

extent to which it is maintained over time. To investigate this, Cos-7 cells were transiently cotransfected with green fluorescent protein (GFP)–Sec61β (a general ER marker) and mCherry-Rab5 (a marker of EEs) and then imaged live by confocal FM to simultaneously visualize the position of EEs relative to the tubular ER membrane network over time (Figure 2A). We analyzed individual Rab5-labeled EEs to determine the degree to which they maintain association with the ER over the time course of a 2-min movie (in the periphery of the cell where tubular ER could be resolved). We show several examples of EEs that either become or remain associated with the ER (Figure 2B and Supplemental Video S4). Many EEs remained associated with the ER throughout the entire movie even though both organelles undergo extensive movements (see examples 1, 2, and 4 in Figure 2B and Supplemental Video S4). These EEs are striking in the way that they remain coupled to the ER network and do not dissociate into the open space between tubules. Some EEs are associated with the ER during part of the movie (see example 3 in Figure 2B and Supplemental Video S4), whereas other EEs are not ER associated at all. We determined the percentage of EEs that fall into each of these three categories by tracking the position of 651 individual EEs (from eight cells) relative to the ER during 2-min movies. These analyses revealed that 50% of EEs (328 of 651) maintained association with the tubular ER network during the course of the entire 2-min movie, whereas 30% (193 of 651) are associated with the ER during part of the movie and 20% (130 of 651) are not ER associated (Figure 2C, right bar). Although the number, distribution, and ER contact of EEs are somewhat variable from cell to cell (Figure 2C, left bars), it is clear that many EEs maintain constant contact with the ER membrane over time. For comparison to another mammalian cell line, we repeated this experiment in U2OS cells and found that 53% of Rab5 EEs maintain association with the ER network during the entire 2-min movie (Supplemental Figure S1). To confirm that the EEs we imaged were functional, we treated cells with fluorescently labeled cargo (transferrin and epidermal growth factor [EGF]) and found that many Rab5-labeled endosomes were able to uptake both cargoes (Supplemental Figure S2, A and B). These data reveal that a large percentage of functional, Rab5-positive EEs are tightly associated with the ER over time.

Late endosomes are more tightly associated with the ER than are EEs

Because of the large extent to which EEs are able to maintain contact with the ER membrane, we next asked whether LEs are similarly able to associate with and move along the ER. LEs are more mature than EEs, are larger than EEs, and are enriched with Rab7 and depleted of Rab5 (for review see Huotari and Helenius, 2011). To measure the association between LEs and the ER, we cotransfected Cos-7 cells with GFP-Rab7 and mCherry-Sec61β (ER) and simultaneously visualized the positions of the two organelles relative to each other over time (Figure 3A). Many LEs localize to the perinuclear region of the cell; however, the ER is very dense in that region, and so we only analyzed the LEs that were in the periphery, where the position of LEs relative to the tubular ER network could be resolved (as in Figure 3B). As with EEs, LEs were categorized as tightly

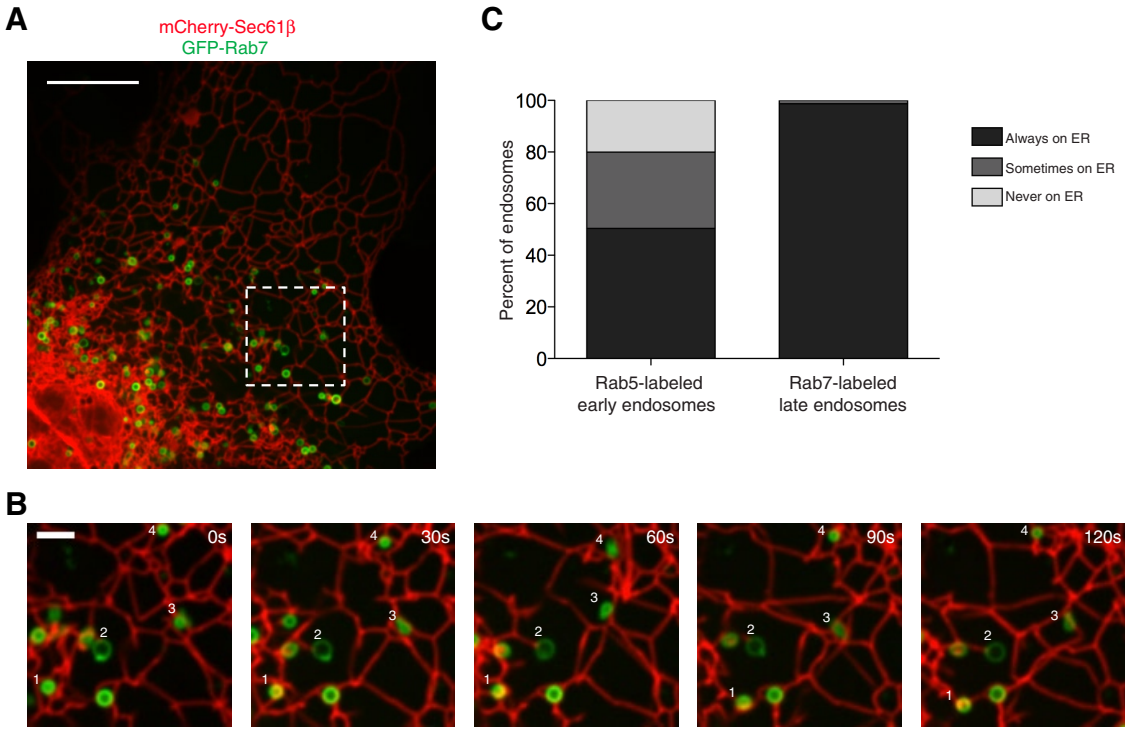

FIGURE 3: Rab7-labeled LEs are tightly associated with the ER membrane. (A) A representative merged image of a Cos-7 cell reveals the distribution of the ER membrane network relative to LEs; labeled with mCherry-Sec61β and GFP-Rab7, respectively). (B) A zoom-in of the dashed box in A over a 2-min time course tracks four endosomes that remain associated with the tubular ER (see Supplemental Video S5). (C) A graph depicting the degree of contact between Rab5$^+$ EEs and the ER (left bar; data from Figure 2C) compared with Rab7$^+$ LEs and the ER (right bar) during 2-min movies imaged every 5 s. The right bar displays data collected from eight cells (n = 224 endosomes). Scale bars, 10 μm (A), 2 μm (B).

associated with the ER if they maintained contact throughout the course of a 2-min movie (see examples in Figure 3B and Supplemental Video S5). Surprisingly, of the 224 individual LEs that we imaged (from eight cells), 99% were tightly associated with the tubular ER network over time. This is much higher than the mean value we found for Rab5-labeled EEs (Figure 3C, compare left and right bars). We measured a similar percentage of LEs (95%) to be tightly associated with the ER membrane in U2OS cells (Supplemental Figure S1). These ER-contacting LEs are functional, as they are competent for fluorescent EGF uptake (Supplemental Figure S2C). These data reveal that LEs are more ER associated than are EEs and, at the resolution of confocal FM, appear to be nearly entirely contacting the ER.

The ER maintains contact with EEs and LEs primarily through ER ring rearrangements

Many Rab5- and almost all Rab7-labeled endosomes maintain contact with the ER over time, yet all three of these organelles are capable of extensive dynamics on MTs. We next sought the mechanism by which the ER maintains its association with endosomes as they move. Our EM data reveal contacts between the ER and endosomes, as well as both organelles contacting MTs. These images suggest that the two organelles might move in a coordinated manner along MTs. Alternatively, dynamic endosomes, particularly Rab5 endosomes, might be more likely to dissociate from the ER membrane as they move. It is possible that the endosomes that maintain contact with the ER over time are those that are relatively immobile. To address this, we first measured whether ER-associated endosomes are dynamic. We defined a dynamic endosome as one that completely leaves a 1-μm-diameter circle drawn around the endosome in the first frame of the movie. Of the 328 EEs that remained tightly associated with the ER during the entire 2-min movie (from Figure 2), 41% were classified as dynamic. We performed a similar analysis on LEs (from Figure 3) and found that 52% of the LEs that are tightly associated with the ER over time are dynamic (Figure 4B). These values might even underreport the dynamics of these endosomes, as we only quantified those we could track throughout the 2-min period. Therefore it seems likely that both EE and LE contacts are associated with some of the dynamic movements that are characteristic of the ER.

ER dynamics can be categorized into three distinct movement types: 1) an ER tubule grows by attaching to the tip of a dynamic MT, 2) an ER tubule travels along the shaft of a stable MT in a motor-dependent manner, or 3) the ER reorganizes by ring rearrangement, which historically refers to the movement, opening, or closure of rings that are typically located at three-way junctions (Lee and Chen, 1988; Waterman-Storer and Salmon, 1998; Wozniak *et al.*, 2009). These last, more complicated rearrangements are also MT dependent, as depolymerization of MTs with nocodazole clearly reduces or abolishes them (Wozniak *et al.*, 2009; Friedman *et al.*, 2010). Because dynamic endosomes maintain contact with the ER even as they move, we asked which type of ER dynamics were most often associated with EE and LE movements. We counted any endosome movements that left a 1-μm circle drawn around the endosome and were continuous in a single direction. We first characterized the 134 dynamic, ER-associated EEs, which together underwent a total of 158 different movements; of these, 150 movement events (95%) were associated with ER rearrangements (Figure 4, A and C, and

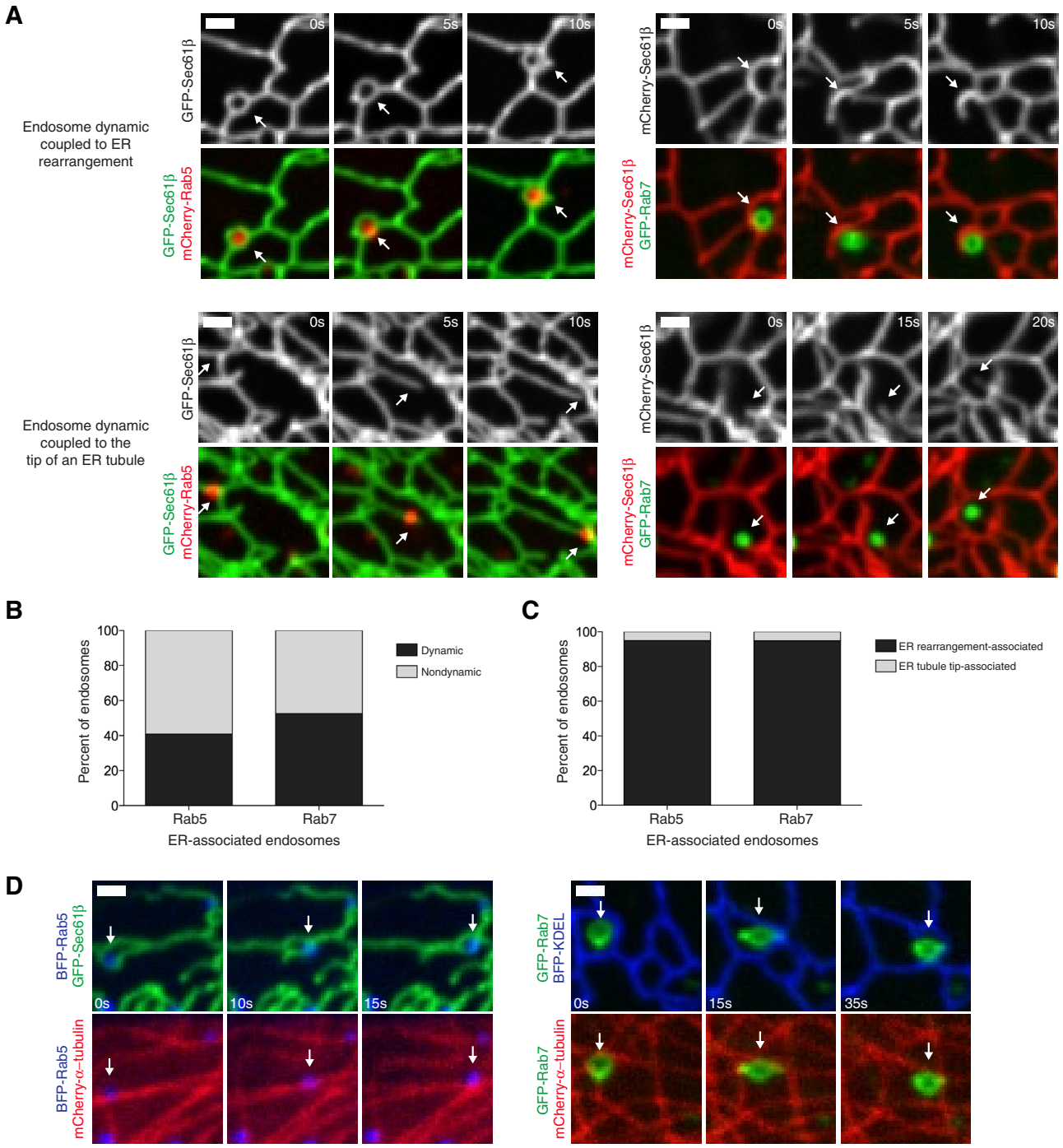

FIGURE 4: The ER maintains contact with dynamic EEs and LEs by ER rearrangement dynamics. (A) Time-lapse examples of the main types of coupled ER-endosome dynamics from Cos-7 cells transfected with GFP-Sec61β (ER) and mCherry-Rab5 (EEs) or mCherry-Sec61β (ER) and GFP-Rab7 (LEs). Top, ER tubules that maintain contact with dynamic EEs (left) and LEs (right) through ring rearrangements (see Supplemental Videos S6 and S7). Bottom, dynamic EEs (left) and LEs (right) that maintain contact with the tip of a growing ER tubule (see Supplemental Videos S8 and S9). Arrows indicate the position of the endosome. (B) A graph depicting the percentage of EEs (left) and LEs (right) that maintain contact with the ER and are dynamic or nondynamic. (C) A graph depicting the percentage of EE (left) and LE (right) movements from endosomes that maintain ER association that are coupled to ER rearrangements and the tips of ER tubules. (D) Examples of dynamic Rab5$^+$ (left) and dynamic Rab7$^+$ (right) endosomes that are coupled to ER rearrangements and move along MTs from Cos-7 cells transfected with mCherry–α-tubulin (MTs) and either GFP-Sec61β (ER) and mCherry-Rab5 or mCherry-Sec61β (ER) and GFP-Rab7. Arrows indicate the position of the endosome. Scale bars, 1 μm.

Supplemental Video S6). Only eight EE dynamics (5%) were associated with the tip of a dynamic ER tubule (Figure 4, A and C, and Supplemental Video S8). We performed a similar analysis on LEs. We analyzed the movements of the 116 ER-associated dynamic LEs, which underwent a total of 212 movements. Of these, 201 (95%) associated with ER rearrangements and 11 (5%) were associated

with the tip of an ER tubule (Figure 4, A and C, and Supplemental Videos S7 and S9). Taken together, these data demonstrate that endosomes maintain contact with the ER despite the dynamics of both organelles, and for both EEs and LEs, this contact is predominantly associated with ER ring rearrangement events.

We next asked whether the endosomes that are coupled to ER ring rearrangements indeed traffic along MTs. Cos-7 cells were transiently transfected with markers for the ER, endosomes, and MTs (using mCherry–α-tubulin) and were imaged live over time to simultaneously image individual organelle dynamic events relative to the MTs. For both Rab5-EEs and Rab7-LEs, we were able to visualize endosome dynamics associated with ER ring rearrangements tracking along MTs. In the examples shown in Figure 4D, both an EE and a LE appear to move directly on MTs while the ER coordinately rearranges its structure to maintain contact with the dynamic endosomes. These data are consistent with our EM models (Figure 1), which show ER wrapped around endosomes and forming contacts with them on multiple sides while both organelles also contact MTs.

Endosome contact with the ER is maintained independent of MTs

Our data show that a large percentage of EEs and the majority of LEs maintain contact with the ER as the organelles traffic along MTs. To address whether the extensive contact between these organelles is secondary to their contact with MTs, we imaged ER–endosome contacts in cells in which MTs were depolymerized. If ER–endosome contact is maintained by direct contact between each organelle, we expect that both EEs and LEs would continue to colocalize with the ER membrane even after MT depolymerization. If instead ER–endosome contact is transient and requires colocalization to MTs to be maintained, then interorganelle contact should be lost after MT depolymerization. Cos-7 cells were cotransfected with markers for the ER and EEs (GFP-Sec61β and mCherry-Rab5) or markers for the ER and LEs (mCherry-Sec61β and GFP-Rab7). The positions of the organelles were imaged relative to each other after treatment with 5 μM nocodazole (for 58 min, as previously described to depolymerize the majority of MTs; Friedman *et al.*, 2010). After imaging in live cells, MT depolymerization was confirmed by fixing, staining the transfected cells with antibody to α-tubulin, and retrospectively imaging them (Supplemental Figure S3, A and B). We first quantified the percentage of Rab5 EEs that were tightly associated with the ER for a 2-min period between 58 and 60 min after nocodazole treatment (Figure 5, A and B). Consistent with the requirement of MTs for trafficking, nocodazole treatment led to a visual increase in the number of small, peripheral, Rab5-labeled endosomes. From regions of four cells, we identified a total of 413 $Rab5^+$ endosomes and found that a similar percentage to our earlier experiments maintain ER association throughout the movie (48% in nocodazole-treated cells vs. 50% in untreated cells; Figure 5E). Of note, after nocodazole treatment, the number of Rab5 endosomes that were sometimes ER associated was greatly decreased, whereas there was a corresponding increase in endosomes that were never ER associated (Figure 5E). These data suggest that a large number of EEs can maintain contact with the ER over time independent of MTs, whereas the population of EEs that are "sometimes ER associated" might be directly contacting the ER to a lesser degree.

We next asked whether LEs can also maintain contact with the ER independent of MTs. We imaged cells expressing markers of the ER and LEs after nocodazole treatment as before (Figure 5, C and D). After nocodazole treatment, Rab7 localized to both LEs with normal appearance, as well as with uncharacteristically small structures that colocalized with Rab5 (Supplemental Figure S3C). Because of this, we quantified both the entire population of Rab7-labeled endosomes and the subset that maintained a "normal" size and shape. From six cells, we identified 430 $Rab7^+$ puncta, of which 79 had a normal appearance. Although the overall population of Rab7 puncta had a somewhat lower ER localization than untreated cells (81% remained tightly ER associated), the majority of normal Rab7 endosomes maintained ER association (92% in nocodazole-treated cells vs. 99% in untreated cells; Figure 5F). These data demonstrate that both EEs and LEs that are tightly ER associated can maintain this contact even in the absence of MTs.

EEs that are more mature are more highly associated with the ER membrane

We were surprised at the extent to which LEs were in contact with the ER compared with EEs. Further, we wondered what could explain the difference between EEs that are and are not tightly associated with the ER. The difference in contact-site stability does not appear to be influenced by the relative dynamics of EEs and LEs, as both can maintain contact with the ER as they move. Instead, the difference in binding could be due to changes that occurred as a result of endosome maturation. EEs in particular encompass a highly heterogeneous population of endosomes that include newly formed endocytic vesicles as well as larger, more mature endosomes that contain intralumenal vesicles and are ultimately destined for degradation by the lysosome (Huotari and Helenius, 2011). Therefore we hypothesized that ER association might be influenced by endosome maturation.

Rab5 is recruited to endosomes soon after they undergo endocytosis at the PM, and, around the same time, the Rab5 effector APPL1 labels these endosomes and is responsible for continued signaling from cargo such as EGF receptor (Miaczynska *et al.*, 2004; Sorkin and von Zastrow, 2009). As these endosomes mature, the membrane lipid phosphatidyl inositol is converted to phosphatidyl inositol 3-phosphate (PI3P) by the PI3P kinase (Huotari and Helenius, 2011). Subsequently, APPL1 dissociates, and the Rab5 effector EEA1, which recognizes PI3P endosomes, is recruited (Zoncu *et al.*, 2009; Figure 6A). Thus APPL1 and EEA1 recognize Rab5-labeled endosomes that are less and more mature, respectively.

To test whether less mature EEs were localized to the ER, we transfected Cos-7 cells with BFP-Sec61β (ER), mCherry-Rab5, and GFP-APPL1 and imaged cells over a 2-min time course (Figure 6B). We identified Rab5 endosomes that were positive for APPL1 and as before, sought extent to which they contact the ER. We imaged the position of 927 individual Rab5 EEs over time relative to the ER membrane network (in seven cells); 819 of these were positive for GFP-APPL1. Of the APPL1-positive endosomes, 57% remained tightly associated with the ER during the entire time course of the movie (Figure 6D). Approximately 10% of the Rab5-labeled endosomes did not colocalize with APPL1; we analyzed these $Rab5^+$/$APPL1^-$ EEs and found that 91% (of these 108 endosomes) were tightly associated with the ER throughout the 2-min movie (Figure 6D). Thus $Rab5^+$/$APPL1^-$ EEs are more ER associated than $Rab5^+$/$APPL1^+$ EEs.

Because maturation of $Rab5^+$ EEs involves exchange of APPL1 for EEA1 (Zoncu *et al.*, 2009), we next tested whether $Rab5^+$/$EEA1^+$ EEs would associate with the ER to a higher degree than the $APPL1^+$ EEs. Cos-7 cells were cotransfected with BFP-Sec61β (ER), mCherry-Rab5, and GFP-EEA1 and visualized live over time (Figure 6C). We analyzed 606 individual Rab5-marked endosomes (from seven cells), and 286 of these labeled positive for EEA1. We found that 86% of $Rab5^+$/$EEA1^+$ EEs are tightly associated with the ER over time and

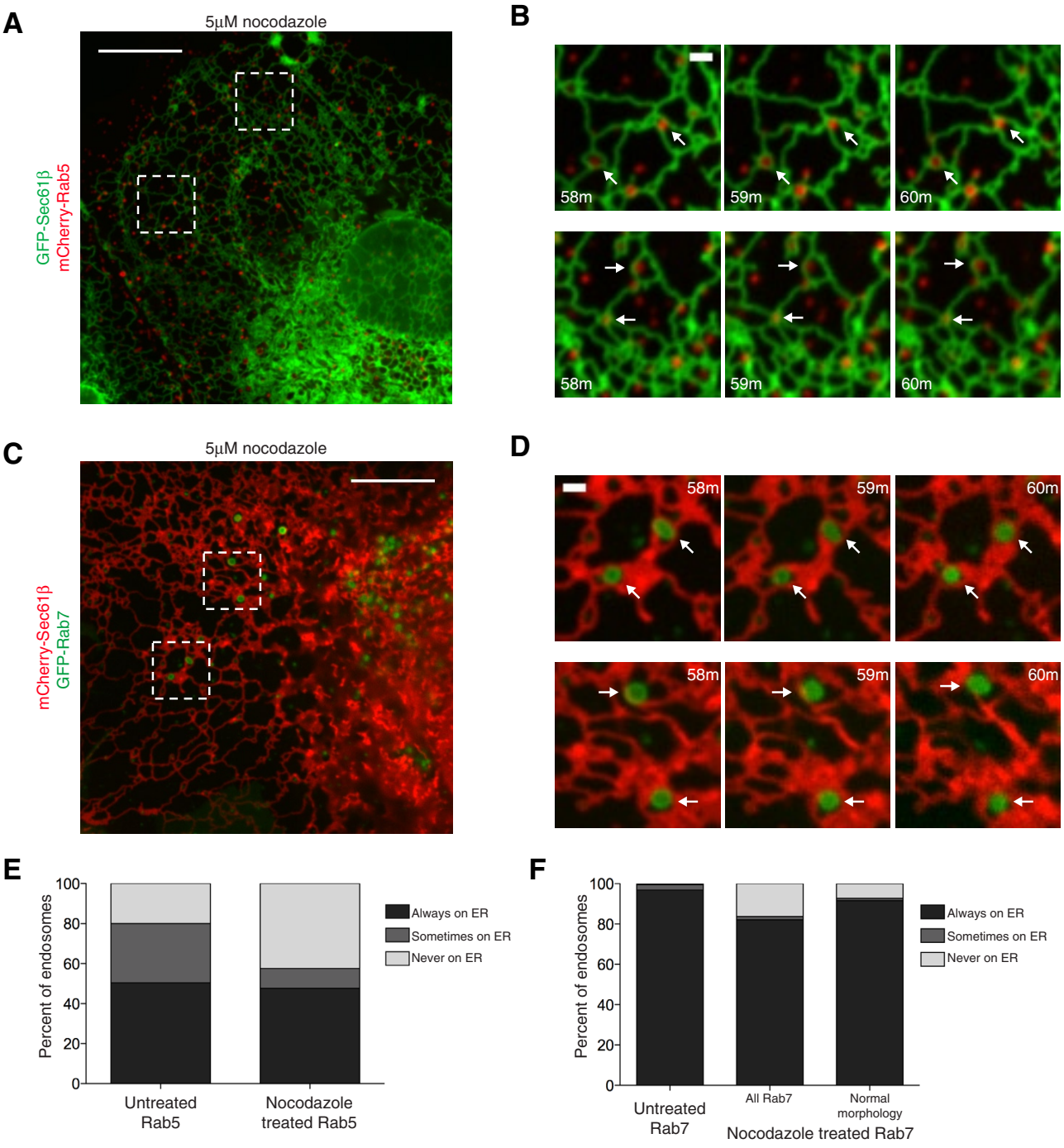

FIGURE 5: ER contact with EEs and LEs is maintained independent of MTs. (A) A single image and (B) zoom-in time-lapse images from dashed boxes from cells transfected with GFP-Sec61β and mCherry-Rab5 and imaged for a 2-min period between 58 and 60 min following 5 μM nocodazole treatment. Arrows mark examples of endosomes that maintain ER contact. (C, D) Cells were transfected with mCherry-Sec61β and GFP-Rab7 and treated as in A and B. Arrows depict Rab7$^+$ endosomes with normal morphology that maintain ER contact. Retrospective images of these cells showing depolymerization of MTs by α-tubulin immunofluorescence are shown in Supplemental Figure S3, A and B. (E) A graph depicting ER localization of Rab5-labeled endosomes before and after nocodazole treatment. The left bar redisplays data from Figure 2. The right bar displays data from four cells imaged from 58 to 60 min after nocodazole treatment (n = 413 endosomes). (F) A graph depicting ER localization of Rab7-labeled endosomes before and after nocodazole treatment. The left bar displays data from Figure 3. The center and right bars display data from six cells imaged from 58 to 60 min after treatment with nocodazole. The center bar depicts all Rab7$^+$ puncta after nocodazole treatment (n = 430), and the right bar depicts Rab7$^+$ endosomes with normal appearance (n = 79). Scale bars, 10 μm (A, C), 1 μm (B, D).

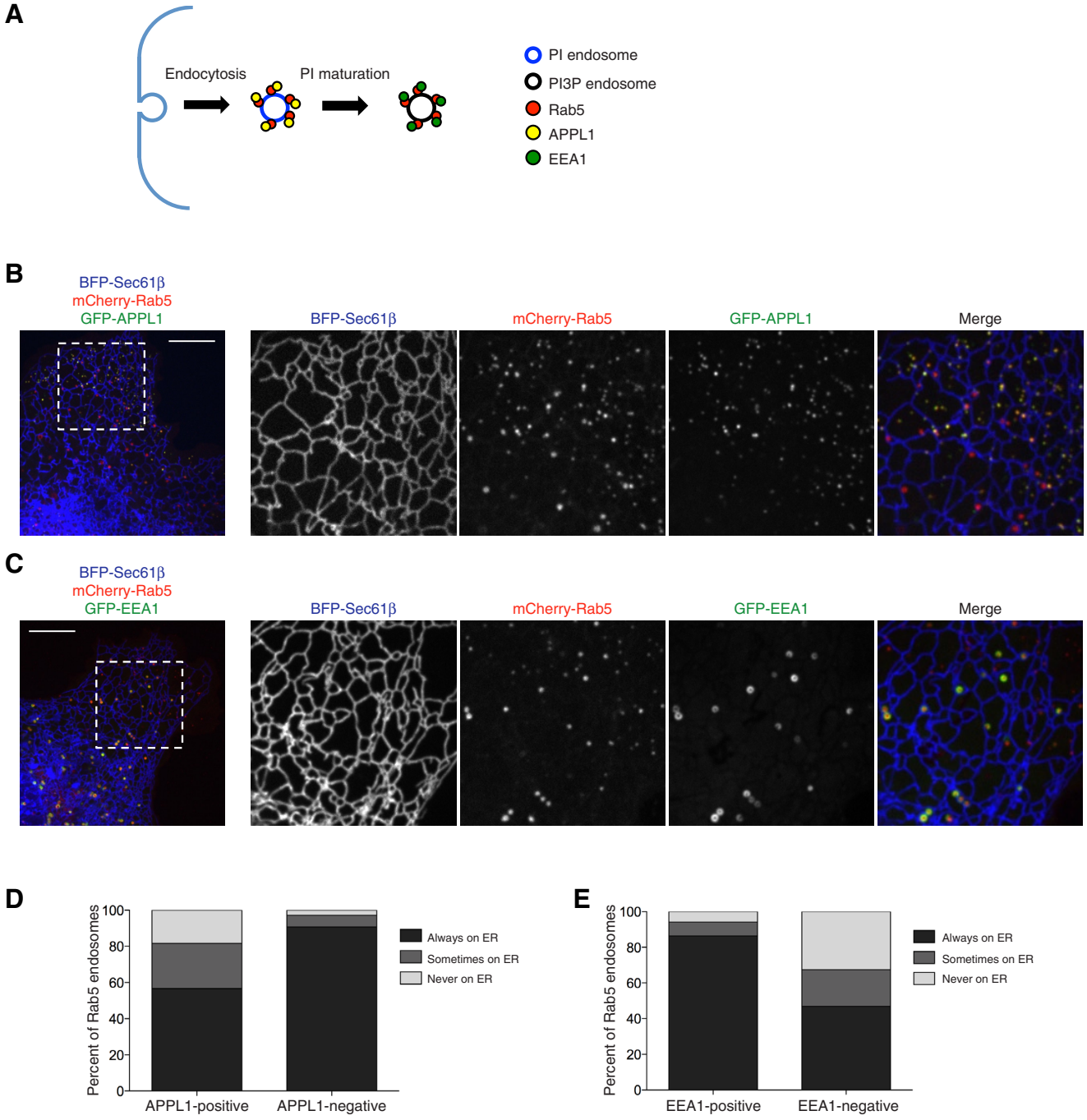

FIGURE 6: EE–ER association increases with endosome maturity. (A) Model depicting the localization of APPL1 to less mature EEs and EEA1 to more mature endosomes. (B) Images from Cos-7 cells transfected with BFP-Sec61β (ER), mCherry-Rab5 (EEs), and GFP-APPL1 show that APPL1$^+$ EEs (yellow in merge) are less ER associated than APPL1$^-$ EEs (remain red in merge). Right, zoom-in of the dashed box shown in the image on left. (C) Images as in B for cells transfected with GFP-EEA1 instead of GFP-APPL1. EEA1$^+$ EEs (yellow in merge) are more ER associated than EEA1$^-$ EEs (red in merge). (D, E) Graphs depict the extent of ER localization of Rab5-labeled EEs that do and do not colocalize with APPL1 (D) and EEA1 (E). Values are the sum of EEs from seven cells for each marker ($n = 927$, D; $n = 606$, E). Scale bars, 10 μm.

only 47% of Rab5$^+$/EEA1$^-$ EEs are tightly associated with the ER (Figure 6E). These data demonstrate that Rab5 EEs that acquire EEA1 are more tightly associated with the ER over time than those containing APPL1. These data reveal that as EEs mature from APPL1$^+$ to EEA1$^+$ endosomes and then ultimately transition to Rab7-marked LEs, each population correspondingly increases its ER association.

Dominant-active Rab5 expression induces enlarged, ER-associated endosomes

Less mature APPL1$^+$ Rab5-EEs are less ER associated than more mature EEA1$^+$ Rab5-EEs. We therefore tested whether promoting Rab5 activity, and thus EE maturity, promoted ER association. A mutation in Rab5 (Q79L) locks Rab5 in its GTP-bound state and acts in a

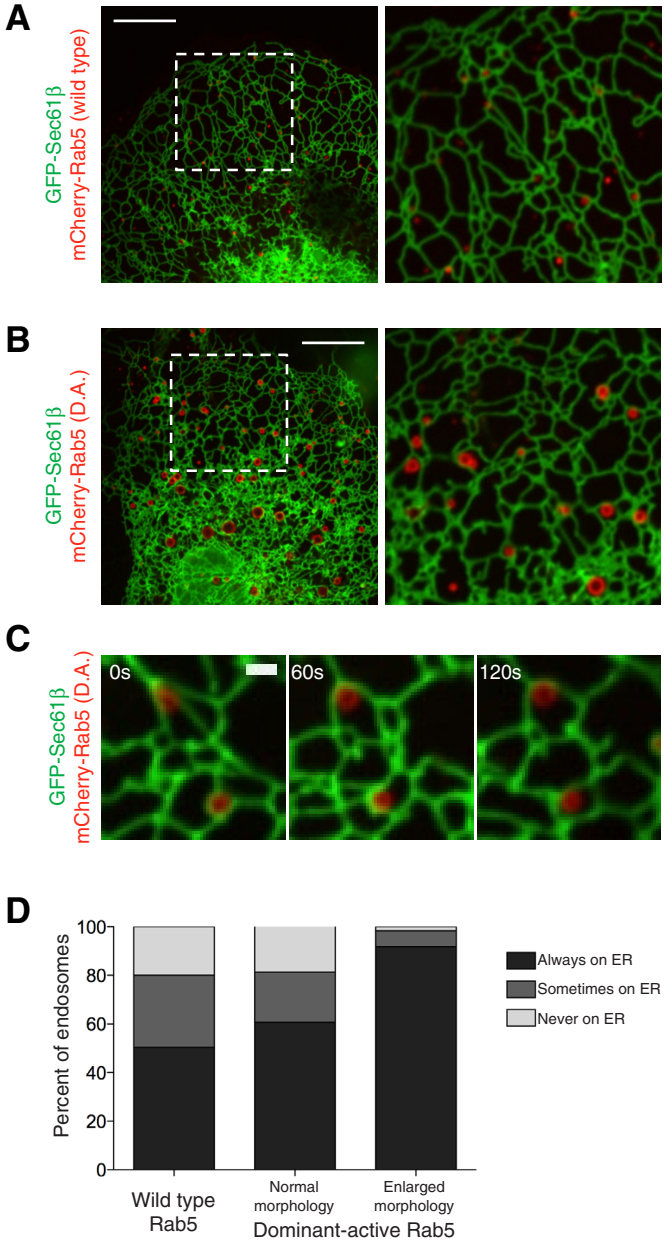

FIGURE 7: Constitutively active Rab5 promotes enlarged EEs that are highly ER associated. (A, B) Images of Cos-7 cells transfected with GFP-Sec61β (ER) and (A) mCherry-Rab5(wild type) or (B) mCherry-Rab5(D.A.) show enlarged endosomes that associate with the ER in the presence of constitutively active Rab5. Left, dashed boxes corresponding to zoom-ins on right. (C) A time-lapse example of enlarged endosomes from cells transfected as in B that remain ER associated. (D) A graph depicting the degree of contact between the ER and endosomes from mCherry-Rab5(D.A.)–expressing cells. The left bar displays data from Figure 2. The center bar depicts normal-sized endosomes ($n = 300$), and the right bar depicts enlarged "halo" endosomes ($n = 183$) from six cells expressing mCherry-Rab5(D.A.). Scale bars, 10 μm (A, B), 1 μm (C).

constitutively active manner (Stenmark *et al.*, 1994). We examined whether expression of this dominant active (D.A.) Rab5 promotes ER association of endosomes. To test this, we transfected Cos-7 cells with GFP-Sec61β (ER) and the Q79L mutant of Rab5, mCherry-Rab5(D.A.). As previously reported, expression of this construct caused the enlargement of EEs compared with wild-type Rab5, causing a "halo" appearance typical of larger LEs (compare Figure 7, A and B; Stenmark *et al.*, 1994). By contrast, enlarged Rab5 endosomes are rarely observed in cells expressing wild-type Rab5. We quantified D.A.-expressing cells with a mix of both enlarged and typical-sized Rab5 endosomes and in which the enlarged endosomes localized to the periphery of the cell, where ER tubules could also be well resolved. We imaged cells during a 2-min time course and tested the degree of ER contact of the enlarged "halo" D.A. Rab5 endosomes. We quantified 183 enlarged and 300 typical-sized endosomes from six cells. Strikingly, the enlarged D.A. Rab5 endosomes were highly ER associated, remaining constitutively ER bound 92% of the time (Figure 7, C and D). By contrast, the normal-sized endosomes in these cells localized to the ER to a similar extent as in cells expressing wild-type Rab5 (60% always ER associated and 21% sometimes ER associated; Figure 7D). Taken together, these data suggest that in cells expressing GTP-locked Rab5, enlarged, more mature endosomes caused by Rab5 hyperactivity are ER associated to a higher degree than the smaller, less mature endosomes in these cells or than in cells expressing wild-type Rab5. These data support the hypothesis that ER contact with endosomes correlates with endosomal maturity.

DISCUSSION

To traffic toward the lysosome, both EEs and LEs are highly dynamic along the MT cytoskeleton. These organelles may couple their movements with the ER to maintain contact. We show here that the majority of endosome movements are associated with ER ring rearrangements and further confirm by EM that these two organelles make extensive contact both with each other and with MTs as a mechanism to ensure that they remain coupled. Thus endosomes traffic along MTs while wrapped in the ER membrane network. These results also reveal that complex ER dynamics such as ring rearrangements could be a direct result of movements of the endosomes to which the ER is attached.

Our data demonstrate that most endosomes are tightly associated with the ER membrane network as they mature and traffic. We show that these interactions increase with the maturity of an endosome. EEs that are marked by APPL1 are associated with the ER to a lesser extent than those that colocalize with EEA1, which recognizes more mature EEs that have accumulated PI3P. Further, promotion of EE maturity by expressing a GTP-locked Rab5 mutant increases ER association of EEs. Meanwhile, endosomes that acquire Rab7, a marker of LEs, are nearly completely and constitutively bound to the ER membrane. Thus, as endosomes mature from newly formed endocytic vesicles to degradative endosomes destined for the lysosome, they associate with and maintain contact with the ER membrane during their journey.

Why are endosomes associated with the ER during their biogenesis? The ER has many useful features that may contribute to endosome biogenesis. There are data that suggest that one function of ER–endosome contact is the transfer of cholesterol (Rocha *et al.*, 2009). In addition, cargo on maturing endosomes may need to be modified by enzymes on the ER membrane (Eden *et al.*, 2010). The ER is also a storage site for Ca^{2+}, and it is possible that there are endosomal factors that require a high concentration of Ca^{2+} found at contact sites. Endosomes may also provide an activity required by the ER. Although factors have been identified that interact between the ER membrane and endosomes, these have not been shown to be required for tethering. The identity of the tethers will be necessary to fully probe the functions of these prevalent contacts and will be of particular interest in testing the role of the ER in endosomal maturation.

MATERIALS AND METHODS

Plasmid construction and use

GFP-Sec61β (Shibata *et al.*, 2008), mCherry-Sec61β (Zurek *et al.*, 2011), BFP-Sec61β (Zurek *et al.*, 2011), BFP-KDEL (Friedman *et al.*, 2011), mCherry-Rab5 (Friedman *et al.*, 2010), and mCherry–α-tubulin (Friedman *et al.*, 2010) were previously described. GFP-Rab7 was described by Choudhury *et al.* (2002) and GFP-APPL1 by Erdmann *et al.* (2007), and both were purchased from AddGene (Cambridge, MA; plasmids 12605 and 22198, respectively). BFP-Rab5 was generated by PCR amplifying human Rab5b (National Center for Biotechnology Information [NCBI] accession number NM_002868.3) and cloning it into the *Xho*I/*Bam*HI sites of pTagBFP-C (Evrogen, Moscow, Russia). GFP-EEA1 was generated by PCR amplifying human EEA1 (NCBI accession number NM_003566.3; contains natural variant K810Q) and cloning it into the *Xho*I/*Bam*HI sites of pAcGFP1-C1 (Clontech, Mountain View, CA). mCherry-Rab5(Q79L) was generated by site-directed mutagenesis. The following amounts of plasmid DNA were transfected into cells for experiments: 1 μg of GFP-Sec61β, BFP-Sec61β, mCherry-Sec61β, and BFP-KDEL; 250 ng of mCherry-Rab5; 250 ng of mCherry-Rab5(Q79L); 125 ng of mCherry–α-tubulin; 100 ng of GFP-Rab7 and GFP-EEA1; 50 ng of BFP-Rab5; and 30 ng of GFP-APPL1.

Cell growth

Cos-7 cells or U2OS cells were grown in DMEM (Invitrogen, Carlsbad, CA) supplemented with 10% fetal bovine serum (Invitrogen) and penicillin/streptomycin. Cells were seeded in a six-well plate at a density of 2×10^5 cells/well ~16 h before transfection. Plasmid DNA transfections were performed for ~5 h in OPTI-MEM media (Invitrogen) in combination with 5 μl of Lipofectamine 2000 according to the manufacturer's instructions. After transfection, cells were reseeded at a density of 1.6×10^5 cells/dish in glass-bottom microscope dishes (MatTek, Ashland, MA), grown for 16–24 h, and imaged in OPTI-MEM media. U2OS cells were plated onto glass-bottom microscope dishes coated with 0.1 mg/ml poly-L-lysine (Sigma-Aldrich, St. Louis, MO).

Confocal microscopy

Cell imaging was performed with an inverted fluorescence microscope (TE2000-U; Nikon, Melville, NY) equipped with an electron-multiplying charge-coupled device (CCD) camera (Cascade II; Photometrics) and a Yokogawa spinning-disk confocal system (CSU-Xm2; Nikon). Images were taken with a 100×/numerical aperture 1.4 oil objective (Nikon), and imaging in live cells was performed at 37°C in a live-cell incubation chamber (Pathology Devices, Westminster, MD). Images were acquired with MetaMorph 7.0 (MDS Analytical Technologies, Sunnyvale, CA), analyzed using ImageJ (National Institutes of Health, Bethesda, MD), and contrasted and merged using Photoshop (Adobe, San Jose, CA). Scale bars were generated using ImageJ. Supplemental videos were generated using ImageJ.

Rab5 and Rab7 ER localization experiments

Cells expressing endosome and ER markers were imaged in a single plane of focus for 2 min with images taken every 5 s. Regions of cells where tubular ER could be resolved and appeared continuous in a single plane of view were analyzed. Endosomes were counted as always ER associated if they remained in contact with the ER during every frame of the movie, partly ER associated if the endosome contacted the ER in some frames of the movie, and not ER associated if no ER contact was visible.

Nocodazole treatment, imaging, and retrospective MT analysis

Posttransfection, cells were seeded to glass-bottom, gridded microscope dishes (MatTek). Before imaging, growth medium was exchanged for OPTI-MEM containing 5 μM nocodazole (Acros Organics, Geel, Belgium). Cells were imaged for a 2-min period between 58 and 60 min of treatment, followed by immediate fixation in phosphate-buffered saline containing 4% paraformaldehyde (Electron Microscopy Sciences, Hatfield, PA) and 0.5% glutaraldehyde (Electron Microscopy Sciences) and permeabilization in 0.1% Triton X-100 (Thermo Fisher, Waltham, MA). Immunofluorescence of MTs was performed with antibody against α-tubulin (Abcam, Cambridge, MA) and with secondary antibody coupled to Alexa Fluor 405 (Invitrogen). Cells were reimaged for ER, Rab5, or Rab7, as well as for MTs, and any endosomes localizing to remaining MTs were excluded from analysis. Owing to the abundance of Rab5-labeled endosomes after nocodazole treatment, we quantified those endosomes in a 20-μm-wide box extending from cell center to cell periphery.

Fluorescent cargo treatment and imaging

Before imaging, cells were treated with fresh growth media containing 1 μg/ml EGF conjugated to Alexa Fluor 647 (Invitrogen) or 50 μg/ml transferrin conjugated to Alexa Fluor 488 (Invitrogen) for 5 min. Cells were washed twice with OPTI-MEM and imaged from 5–15 min after washout (for colocalization with Rab5) or 35–45 min after washout (for colocalization with Rab7).

Electron microscopy

Cos-7 cells were grown on carbon-coated sapphire disks and high pressure frozen with a Bal-Tec HPM 010 machine in 0.025-mm-depth by 3-mm aluminum specimen carriers (TechnoTrade, Manchester, NH) in culture media containing 10% Ficoll. The sapphire disks were transferred to an automated freeze substitution unit (Leica, Wetzlar, Germany), warmed to −90°C, dehydrated in distilled acetone, and fixed in 0.1% uranyl acetate and 0.25% glutaraldehyde (McDonald *et al.*, 2010). Cells were then washed in acetone, warmed to −60°C, and infiltrated with Lowicryl HM20 (Polysciences, Warrington, PA; adapted from Hawes *et al.*, 2007). The cells were then ultraviolet polymerized at −60°C for 96 h, the sapphire disks were removed, and the blocks were en face sectioned to 200 nm using an ultramicrotome (Leica) and collected onto 1% Formvar films adhered to rhodium-plated copper grids (Electron Microscopy Sciences). Grids were labeled on both sides with fiduciary 15-nm colloidal gold (British Biocell International, Cardiff, United Kingdom). Dual-axis tilt series were collected from ±60° with 1° increments using serial EM (Mastronarde, 1997) at 200 kV using a Tecnai 20 FEG electron microscope (FEI, Hillsboro, OR). Negative defocus equivalent to the sample thickness (~250 nm) was used after autofocus to increase the phase contrast component. Tilt series were recorded at a magnification of 19,000× using serial EM (Mastronarde, 2005). After 2× binning on the recording 4 × 4K CCD camera (Gatan, Pleasanton, CA), a 2 × 2K image was created with a pixel size of 1.51 nm. Dual-axis electron tomograms were built using the IMOD software package (Kremer *et al.*, 1996). ER, endosomal limiting membrane, MTs, and ER–endosomal contact surfaces were manually assigned contours using 3DMOD and imodmesh (3DMOD 4.0.11). Supplemental videos were made from IMOD images and completed in QuickTime Pro 7.5 (Apple, Cupertino, CA). Endosomes modeled in Figure 1 are from two different wild-type, untransfected Cos-7 cells.

ACKNOWLEDGMENTS

We thank T. Giddings, M. Ladinsky, M. Morphew, and J. Martin for contributing to the adaptation of cryofixation EM methods and A. Hoenger and the Boulder Lab for 3D Electron Microscopy for shared equipment and helpful suggestions. We thank A. English for helpful suggestions, J. Nunnari for critical reading of the manuscript, and R. Pagano and P. De Camilli for generating plasmids used here. This work was supported by National Institutes of Health Grant GM083977 to G.V. and Predoctoral Grants GM08759 and GM07135 to J.F. and A.R., respectively. J.D. was supported by grants from the Howard Hughes Medical Institute Undergraduate Research Opportunity Program and the Biological Sciences Initiative at the University of Colorado Boulder.

REFERENCES

Choudhury A, Dominguez M, Puri V, Sharma DK, Narita K, Wheatley CL, Marks DL, Pagano RE (2002). Rab proteins mediate Golgi transport of caveola-internalized glycosphingolipids and correct lipid trafficking in Niemann-Pick C cells. J Clin Invest 109, 1541–1550.

Eden ER, White IJ, Tsapara A, Futter CE (2010). Membrane contacts between endosomes and ER provide sites for PTP1B-epidermal growth factor receptor interaction. Nat Cell Biol 12, 267–272.

Erdmann KS, Mao Y, McCrea HJ, Zoncu R, Lee S, Paradise S, Modregger J, Biemesderfer D, Toomre D, De Camilli P (2007). A role of the Lowe syndrome protein OCRL in early steps of the endocytic pathway. Dev Cell 13, 377–390.

Friedman JR, Lackner LL, West M, DiBenedetto JR, Nunnari J, Voeltz GK (2011). ER tubules mark sites of mitochondrial division. Science 334, 358–362.

Friedman JR, Webster BM, Mastronarde DN, Verhey KJ, Voeltz GK (2010). ER sliding dynamics and ER-mitochondrial contacts occur on acetylated microtubules. J Cell Biol 190, 363–375.

Hawes P, Netherton CL, Mueller M, Wileman T, Monaghan P (2007). Rapid freeze-substitution preserves membranes in high-pressure frozen tissue culture cells. J Microsc 226, 182–189.

Huotari J, Helenius A (2011). Endosome maturation. EMBO J 30, 3481–3500.

Kremer JR, Mastronarde DN, McIntosh JR (1996). Computer visualization of three-dimensional image data using IMOD. J Struct Biol 116, 71–76.

Lee C, Chen LB (1988). Dynamic behavior of endoplasmic reticulum in living cells. Cell 54, 37–46.

Mastronarde DN (1997). Dual-axis tomography: an approach with alignment methods that preserve resolution. J Struct Biol 120, 343–352.

Mastronarde DN (2005). Automated electron microscope tomography using robust prediction of specimen movements. J Struct Biol 152, 36–51.

McDonald K, Schwarz H, Muller-Reichert T, Webb R, Buser C, Morphew M (2010). Tips and tricks" for high-pressure freezing of model systems. Methods Cell Biol 96, 671–693.

Miaczynska M, Christoforidis S, Giner A, Shevchenko A, Uttenweiler-Joseph S, Habermann B, Wilm M, Parton RG, Zerial M (2004). APPL proteins link Rab5 to nuclear signal transduction via an endosomal compartment. Cell 116, 445–456.

Nielsen E, Severin F, Backer JM, Hyman AA, Zerial M (1999). Rab5 regulates motility of early endosomes on microtubules. Nat Cell Biol 1, 376–382.

Poteryaev D, Datta S, Ackema K, Zerial M, Spang A (2010). Identification of the switch in early-to-late endosome transition. Cell 141, 497–508.

Rink J, Ghigo E, Kalaidzidis Y, Zerial M (2005). Rab conversion as a mechanism of progression from early to late endosomes. Cell 122, 735–749.

Rocha N, Kuijl C, van der Kant R, Janssen L, Houben D, Janssen H, Zwart W, Neefjes J (2009). Cholesterol sensor ORP1L contacts the ER protein VAP to control Rab7-RILP-p150 Glued and late endosome positioning. J Cell Biol 185, 1209–1225.

Shibata Y, Voss C, Rist JM, Hu J, Rapoport TA, Prinz WA, Voeltz GK (2008). The reticulon and DP1/Yop1p proteins form immobile oligomers in the tubular endoplasmic reticulum. J Biol Chem 283, 18892–18904.

Sorkin A, von Zastrow M (2009). Endocytosis and signalling: intertwining molecular networks. Nat Rev Mol Cell Biol 10, 609–622.

Stenmark H (2009). Rab GTPases as coordinators of vesicle traffic. Nat Rev Mol Cell Biol 10, 513–525.

Stenmark H, Parton RG, Steele-Mortimer O, Lutcke A, Gruenberg J, Zerial M (1994). Inhibition of rab5 GTPase activity stimulates membrane fusion in endocytosis. EMBO J 13, 1287–1296.

Stuible M, Tremblay ML (2010). In control at the ER: PTP1B and the down-regulation of RTKs by dephosphorylation and endocytosis. Trends Cell Biol 20, 672–679.

Vonderheit A, Helenius A (2005). Rab7 associates with early endosomes to mediate sorting and transport of Semliki forest virus to late endosomes. PLoS Biol 3, e233.

Waterman-Storer CM, Salmon ED (1998). Endoplasmic reticulum membrane tubules are distributed by microtubules in living cells using three distinct mechanisms. Curr Biol 8, 798–806.

West M, Zurek N, Hoenger A, Voeltz GK (2011). A 3D analysis of yeast ER structure reveals how ER domains are organized by membrane curvature. J Cell Biol 193, 333–346.

Wozniak MJ, Bola B, Brownhill K, Yang YC, Levakova V, Allan VJ (2009). Role of kinesin-1 and cytoplasmic dynein in endoplasmic reticulum movement in VERO cells. J Cell Sci 122, 1979–1989.

Zeigerer A *et al*. (2012). Rab5 is necessary for the biogenesis of the endolysosomal system in vivo. Nature 485, 465–470.

Zoncu R, Perera RM, Balkin DM, Pirruccello M, Toomre D, De Camilli P (2009). A phosphoinositide switch controls the maturation and signaling properties of APPL endosomes. Cell 136, 1110–1121.

Zurek N, Sparks L, Voeltz G (2011). Reticulon short hairpin transmembrane domains are used to shape ER tubules. Traffic 12, 28–41.